ELSEVIER

Thermochimica Acta 327 (1999) 173–180

thermochimica acta

Thermal decomposition of freeze-dried μ-oxo-carboxylates of manganese and iron

H. Langbein*, S. Christen, G. Bonsdorf

Institute of Inorganic Chemistry, Dresden University of Technology, Mommsenstr. 13, D-01062, Dresden, Germany

Received 2 October 1998; received in revised form 16 November 1998; accepted 18 November 1998

Abstract

The decomposition of freeze-dried mixed carboxylates of manganese and iron was investigated by means of DTA, TG, mass spectroscopy and X-ray powder diffractometry. The three main steps of decomposition are characterized as release of (a) H_2O, (b) carboxylic acid and CO_2/CO, and (c) the corresponding carbonyl compound and CO_2. In particular, the course of process (b) strongly depends on the stability of the metal–carboxylate link in the three investigated carboxylates. Well-crystallized single-phase manganese ferrites can be obtained on decomposition of formates of appropriate composition and thermal treatment of decomposition products at 600°C while maintaining a $p(O_2)$ within the coexistence field of manganese ferrite.

Keywords: Manganese ferrite; Freeze-dried precursor; Thermal decomposition; Thermal analysis; Mass spectroscopy

1. Introduction

Trinuclear μ-oxo-carboxylates $Fe_2(III)M(II)O(RCOO)_6L_3$ (R = alkyl, H; L = H_2O, RCOOH, M = Zn, Co, Fe, Ni, Mn) are characterized by the metal-ion stoichiometry of spinels on the molecular level. The thermal decomposition of these compounds proceeds in the temperature interval from 40° to 400°C [1]. From this point of view, the trinuclear carboxylates should be suitable precursors for the soft synthesis of ferrites, MFe_2O_4, with spinel structure. Some investigations in this field have shown that thermal decomposition of appropriate μ-oxo-carboxylates leads to spinel ferrites but, in most cases, more or less single oxides are formed [2–4]. The phase composition of the solid products strongly depends on the nature of precursor compounds and the thermal treatment. The main reason for the different results seems to be the difficult synthesis of compounds with an exact Fe : M-stoichiometry. The conditions for a reproducible synthesis are known only for a few sufficient less soluble μ-oxo-acetates [5–7]. Because of these difficulties, we have developed a freeze-drying method for synthesis of reactive amorphous acetates with any M : Fe-stoichiometry. The freeze-dried precursors show a decomposition pathway analogous to the crystalline μ-oxo-acetates of appropriate composition [8,9].

This paper deals with the effect of the nature of the carboxylate anion (formate, acetate, propionate) on the thermal decomposition of freeze-dried Mn–Fe-carboxylates. Common features and differences in the decomposition behaviour are discussed. The most

*Corresponding author. Tel.: +49-0351-463-4366; fax: +49-0351-463-7287; e-mail: Hubert.Langbein@chemie.tu.dresden.de

0040-6031/99/$ – see front matter
PII: S0040-6031(98)00611-X

suitable formates were also investigated in regard to the phase formation in the solid products. Because of the strong influence of the reaction gas atmosphere on the oxidation states of iron and manganese, the $p(O_2)$ was measured continuously with the help of solid electrolyte cells.

2. Experimental

The complex carboxylate solutions for the freeze-drying process were obtained as follows: Mn(II)- and Fe(II)-carboxylates were prepared by dissolving the metal powders in the appropriate carboxylic acid in an inert atmosphere. After that, the Fe(II)-carboxylate was oxidized in a 10^{-2}–10^{-1} M solution of the appropriate carboxylic acid with a twofold excess of H_2O_2. A deep brown Fe(III)carboxylate solution was formed. The maximum attainable concentrations are 0.2 M (formate), 0.6 M (propionate) and 1 M (acetate). An adequate quantity of the appropriate Mn(II)carboxylate solution was added to 500 ml of the Fe(III)carboxylate solution. The mixture was quickly frozen in liquid nitrogen. The drying process was carried out in a vacuum chamber of a freeze-drying apparatus (Christ) from −40 to +20°C at 10^{-3} mbar. The composition of the fine-grained, soft agglomerated powders were determined by complexometric titration and elemental analysis as follows:

$$MnFe_2O(HCOO)_6(H_2O)_3$$

$$MnFe_2O(CH_3COO)_5OH(H_2O)$$

$$MnFe_2O(C_2H_5COO)_6(H_2O)_3$$

Depending on the conditions during the freeze-drying process, the water and carboxylic acid content can be somewhat different. The analysis of the IR spectra allows the conclusion that in the freeze-dried amorphous products at the very least partially complex trinuclear μ-oxo-carboxylate species are present.

The thermal decomposition was investigated by means of a Netzsch thermal analyzer STA 409, coupled with a mass spectrometer QMS 125 (Balzers). X-ray diffraction was performed using a powder diffractometer D5000 (Siemens). The experimental arrangement shown in Fig. 1 was used for the continuous measurement of $p(O_2)$ throughout the thermal decomposition. The ZrO_2-based solid electrolyte cells, C1 and C2, were calibrated with gas mixtures of known $p(O_2)$.

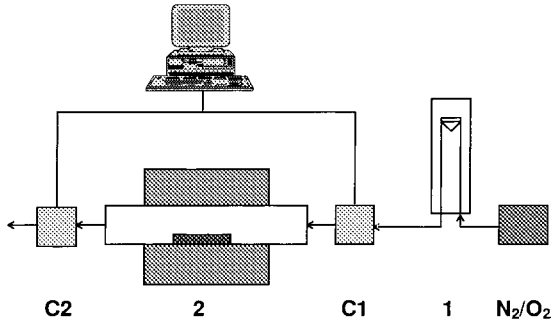

Fig. 1. Experimental arrangement for continuous $p(O_2)$ measurement during decomposition. C1, C2, represent solid electrolyte cells, working temperature 600°C. 1, flow meter; 2, furnace; and N_2 gas flow 10 l/h.

3. Results and discussion

Fig. 2 shows the TG curves of the freeze-dried Fe–Mn-formate, Fe–Mn-acetate and Fe–Mn-propionate. In an inert atmosphere, all the decomposition processes are endothermic. Decomposition takes place in three separate main steps. The mass spectroscopic analysis of gaseous products allows the conclusion that these steps represent five somewhat superimposed decomposition processes. The temperature ranges for these processes and the appropriate main primary gaseous decomposition products are listed in Table 1. Fig. 3(a and b) illustrate the mass spectroscopic analysis for the freeze-dried formate in a more detailed form. Instead of the also observed molecule peaks of HCOOH ($m = 46$) and H_2CO ($m = 30$), the more intensive fragment peaks of COOH ($m = 45$) and HCO ($m = 29$) are shown. For all the investigated carboxylates the decomposition is almost complete at ca. 350°C. The solid decomposition products of acetates and propionates contain, respectively, 1–3% carbon formed by pyrolytic side reactions. In an oxygen containing atmosphere, this carbon is oxidized at ca. 600°C.

The decomposition starts with the elimination of coordinated H_2O (process 1). In case of acetate and propionate, the H_2O elimination is superimposed by the elimination of carboxylic acid. This process, 2(a), can be understood as a thermal hydrolysis of a metal–

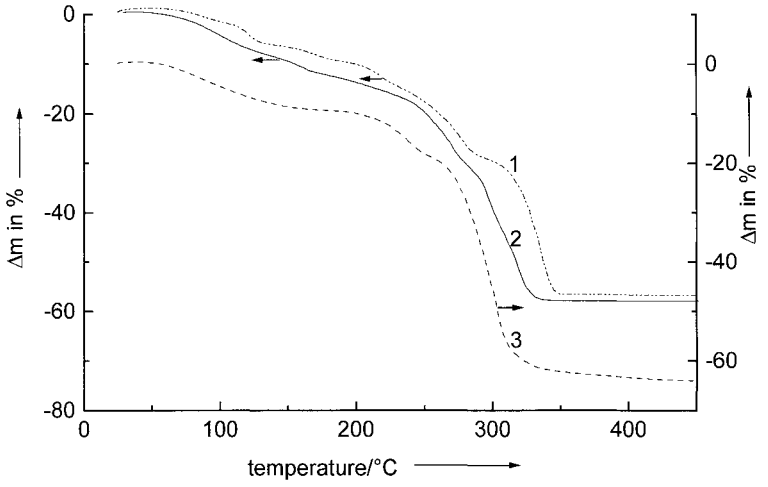

Fig. 2. Thermal analysis of the freeze-dried Mn–Fe-carboxylates. Heating rate 5 K min^{-1}; atmosphere, argon; 1, formate; 2, acetate; and 3, propionate.

O(CO)R-link without alteration of the oxidation number of metal ions. On the contrary, the elimination of formic acid begins only after the end of the delivery of H_2O (process 2(b)). Formic acid originates in an elimination of two HCOO-moieties connected with the reduction of Fe(III) to Fe(II) and an H-transfer process from one moiety to the other (2 HCOO→ HCOOH+CO_2). In case of acetates and propionates, an analogous reductive elimination process also begins at ca. 200°C. The simultaneous formation of carboxylic acid and CO_2 needs the additional formation of CH_2 and C_2H_4. An indirect proof of the reactive CH_2 species is the mass spectroscopic detection of propanoic acid during the decomposition of the freeze-dried acetate. Propanoic acid can arise by a characteristic insertion reaction of CH_2 in a C–H-link of acetic acid.

Following the reduction of Fe(III) to Fe(II), carboxylic acid is released together with CO instead of CO_2. In case of acetates and propionates this process 2(c) is completely superimposed with process 2(b) and partially superimposed with process 3. On the other hand, in case of formate the decomposition processes 2(b) and 2(c) can be observed separately but the processes 2(c) and 3 are completely superimposed.

The results of the decomposition of the formate sample are summarized in Fig. 4. The mass losses observed by TG analysis correlate with the process steps in the reaction scheme. The given formulas for the decomposition products represent only the composition. It must be supposed that after the dehydration reaction all processes are cross-linkages of molecular species forming M–O–M bridges. As in any thermal decomposition involving reactions between primary gaseous products and solids or gas-phase reactions, the actual yield in each reaction product is very sensitive to experimental conditions (heating rate, gas flow, sample mass).

According to Dollimore and Tonge [10], there are two main routes for the decomposition of anhydrous metal formates to oxides:

$$M(OOCH)_2 \rightarrow MO + 2CO + H_2O \quad (1)$$

$$M(OOCH)_2 \rightarrow MO + CO + CO_2 + H_2 \quad (2)$$

The authors refer to the formation of different organic byproducts (for instance H_2CO) depending on reaction conditions. In the case of manganous formate, the gas evolution analysis suggests that at the beginning of decomposition the reaction (1) is favoured kinetically, but gradually assumes less importance in comparison to reaction (2). This result seems to be contradictory to our results, but considering the different reaction conditions the difference can be understood. The main results in [10] were obtained in time-dependent experiments at ϑ>400°C without variation in the oxidation number of metal ions. The lower temperature in our experiments allows the detection of pri-

Table 1
Primary gaseous decomposition products of freeze dried $MnFe_2$-carboxylates

Formate				Acetate			Propionate		
process	temperature range/°C	ϑ_{max}/°C	products	temperaturerange/ °C	ϑ_{max}/°C	products	temperature range/ °C	ϑ_{max}/°C	products
1	70–200	112	H_2O	70–200	140	H_2O	70–200	110	H_2O
2a				110–210	150	CH_3COOH	100–180	140	C_2H_5COOH
2b	200–290	270	HCOOH, CO_2	210–300	265	CH_3COOH, CO_2	180–280	251	C_2H_5COOH, CO_2
2c	260–350	324	HCOOH, CO	210–300	265	CH_3COOH, CO	180–280	251	C_2H_5COOH, CO
3	260–350	324	HCOH, CO_2	250–330	300	CH_3COCH_3, CO_2	260–330	293	$C_2H_5COC_2H_5$, CO_2

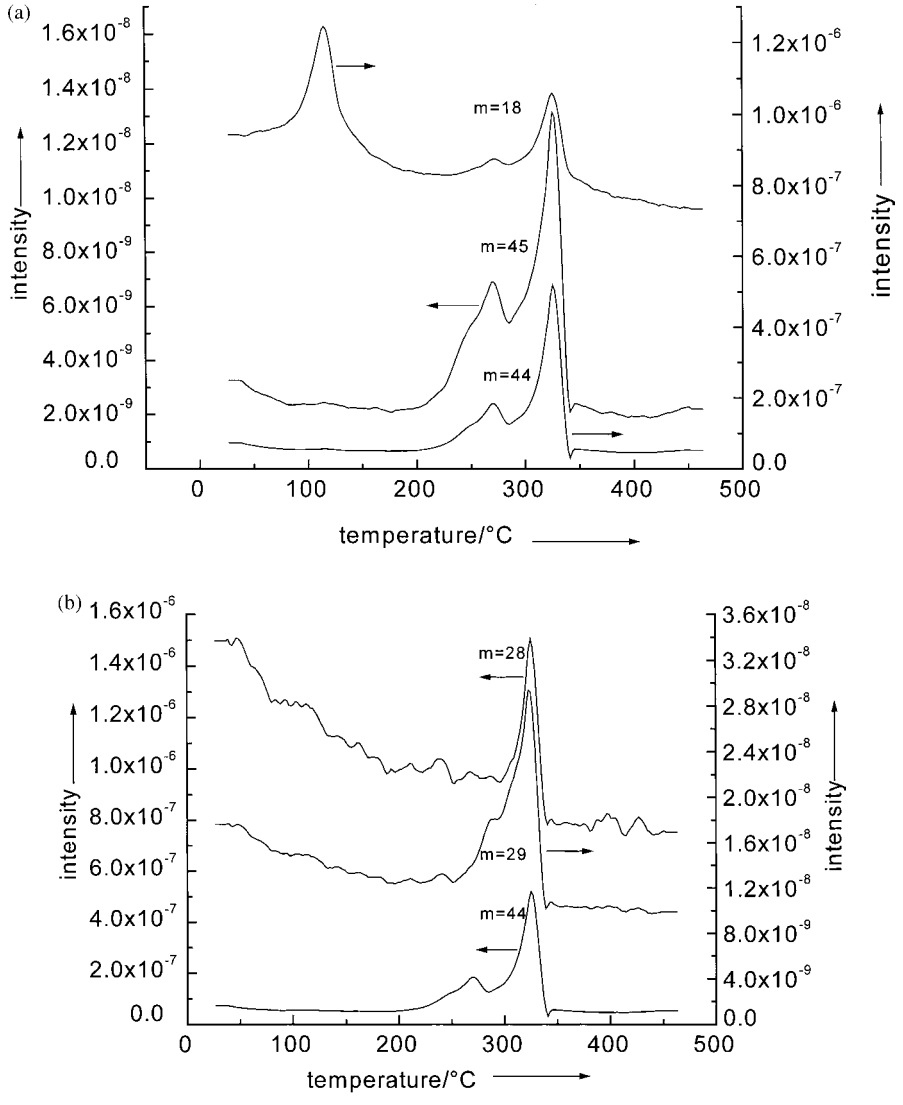

Fig. 3. Observation of mass numbers during the decomposition of the formate precursor. (a) $m = 18$, H_2O; $m = 44$, CO_2; $m = 45$, HCOO fragment; and (b) $m = 28$, CO; $m = 29$, HCO fragment; and $m = 44$, CO_2.

mary gaseous products HCOOH and H_2CO as main components besides CO, CO_2, H_2O and H_2 which are also observed. Because of the reductive decomposition step 2(b), CO_2 instead of CO is formed at first in addition to HCOOH. Decomposition of HCOOH takes place already below 300°C in accordance with Eqs. (3) and (4).

$$HCOOH \rightarrow H_2 + CO_2 \quad (3)$$

$$HCOOH \rightarrow H_2O + CO \quad (4)$$

Independent of kinetic influences, the exothermic reaction (3) should gradually assume less importance with rising temperature, unlike the endothermic reaction (4). The absence of CO below 300°C can also be explained by the consecutive reaction (5).

$$CO + HCOOH \rightarrow CO_2 + H_2CO \quad (5)$$

The shoulder in the intensity graph of the fragment peak with $m = 29$ at ca. 280°C (Fig. 3(b)) refers to this reaction.

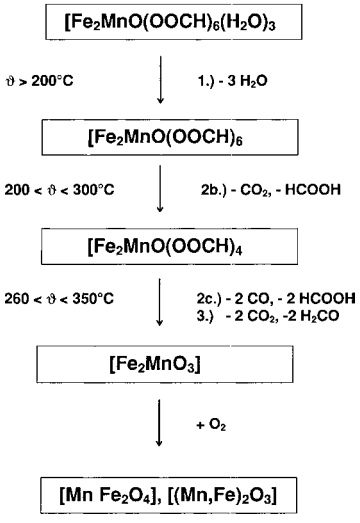

Fig. 4. Decomposition scheme for Mn–Fe-formate.

After finishing the reductive elimination, the formation of HCOOH is connected with the release of CO (process 2(c)). Taking into account the consecutive reaction (4), the whole process fully corresponds to reaction (1).

In a completely overlapped reaction 3 (Table 1 and Fig. 4) CO_2 and H_2CO are formed. Decomposition of H_2CO, according to Eq. (6)

$$H_2CO \rightarrow H_2 + CO \tag{6}$$

results in a reaction corresponding to Eq. (2).

Traces of oxygen in the gas flow cause a minor importance of the reductive elimination of formic acid and, in agreement with this fact, the formation of Mn(II)–Fe(III)-oxide. Decomposition in air atmosphere results in the formation of α-$(Fe,Mn)_2O_3$.

In an atmosphere poor in oxygen, the $p(O)_2$ above the sample in the course of decomposition is determined by the released gaseous products. Fig. 5 represents the results of a continuous measurement of $p(O_2)$ during the decomposition of a freeze-dried formate in an arrangement shown in Fig. 1. The dotted area designates the oxygen coexistence pressure for single-phase spinels $MnFe_2O_{4\pm\delta}$ at 600°C. The upper and lower $p(O_2)$ were calculated according to the hypothetic coexistences (7) and (8) using thermodynamic data of Barin [11].

$$2Mn_3O_4 + 6Fe_2O_3 \rightleftarrows 6MnFe_2O_4 + O_2 \tag{7}$$

$$6MnFe_2O_4 \rightleftarrows 6MnO + 4Fe_3O_4 + O_2 \tag{8}$$

We have shown that this approximation is sufficiently exact for the determination of preparation conditions for manganese ferrite [12]. Actually, the

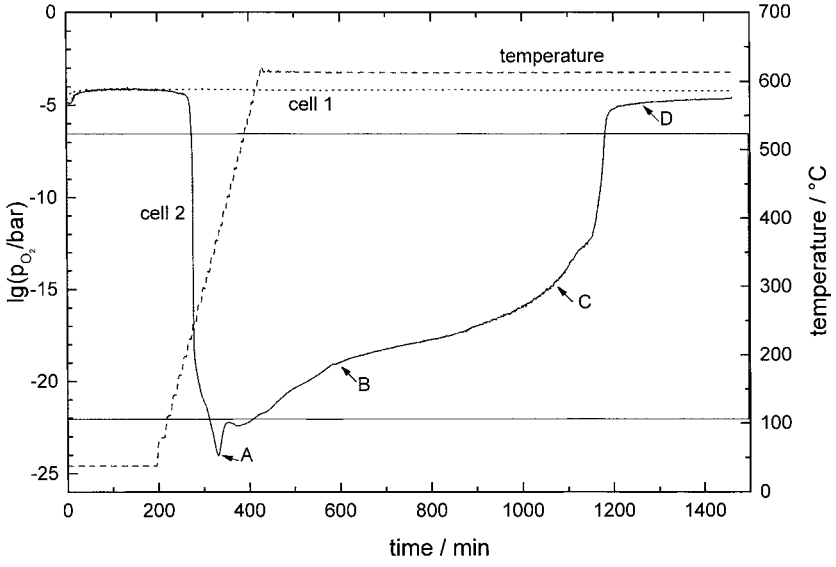

Fig. 5. Analysis of $p(O_2)$ during the thermal treatment of the Mn–Fe-formate precursor. Dotted area, oxygen coexistence pressures for single-phase spinels $MnFe_2O_{4\pm\delta}$ at 600°C; cell 1, $p(O_2)$ at C1; cell 2, $p(O_2)$ at C2 (see Fig. 1).

reduction of Fe(III) in $MnFe_2O_4$ at the lower phase boundary, first of all, results in the formation of an Fe-rich spinel, ($Mn_{1-x}^{2+}Fe_x^{2+}Fe_2^{3+}O_4$), besides an Mn-rich manganowüstite phase ($Mn_{1-y}Fe_yO$). At the upper phase boundary the oxidation of Mn(II) firstly leads to the formation of an Mn-rich spinel ($Mn^{2+}Mn_{2-x}^{3+}Fe_x^{3+}O_4$) and an Fe-rich α-(Fe,-Mn)$_2O_3$.

The oxygen content in the N_2 gas stream before the sample is held constantly and measured with the solid electrolyte cell C1 as $p(O_2) = 10^{-4}$ bar. Below a sample temperature of 200°C, the same oxygen partial pressure in the gas stream is measured at cell C2 after passing the sample. Above 200°C, the $p(O_2)$ measured at C2 decreases because of the reaction of gaseous decomposition products with traces of oxygen in the gas stream. At point A in Fig. 5, the decomposition is finished and the released gases are outside the reaction zone. In correspondence with the above-mentioned assumption, the X-ray powder diffractogram of the solid A demonstrates the presence of a wüstite phase beside a spinel phase (Fig. 6). When the $p(O_2)$ is measured at C2 over a long period, it continuously increases and reaches the original value measured at C1 after a duration of more than 24 h. The local minimum at ca. 380 min/550°C is probably originated by the oxidation of traces of pyrolysis carbon. The further consumption of oxygen is due to the slow oxidation of the solid decomposition product. This is confirmed by the X-ray analysis of samples taken at B, C and D (Fig. 6). The portion of spinel phase $MnFe_2O_4$ in the sample B is noticeably higher than this portion at A. After a reaction time corresponding to point C, a single-phase manganese ferrite spinel is obtained. In view of the small phase width $\Delta\delta$ in $MnFe_2O_{4\pm\delta}$ after point C, the $p(O_2)$ measured at C2 quickly increases to a value higher than the coexistence pressure at the upper phase boundary of manganese ferrite. As a consequence, sample D already contains some α-Fe_2O_3 or an Fe-rich α-(Fe,Mn)$_2O_3$ phase. Because of the very low oxygen content in the gas stream, the complete formation of equilibrium phases containing only Mn(III) needs a very long reaction time.

4. Conclusions

Thermal decomposition of freeze-dried complex carboxylates of Mn and Fe is a suitable pathway to synthesize manganese ferrites with spinel structure. Well-crystallized single-phase ferrites can be obtained already on decomposition of formates of appropriate composition and thermal treatment of decomposition products at 600°C, maintaining a $p(O_2)$ within the coexistence field of manganese ferrite.

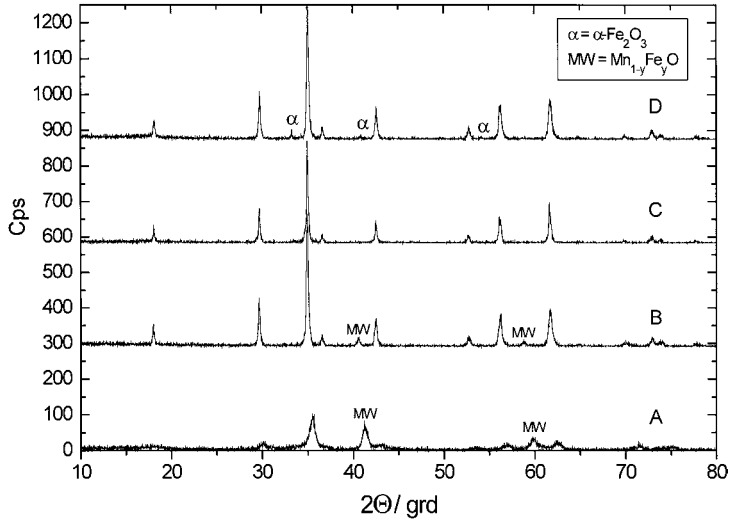

Fig. 6. X-ray powder diffractograms of solid decomposition products (formate precursor). Sampling after a thermal treatment corresponding to points A, B, C and D (see Fig. 5).

The thermal stability of precursors decreases in the sequence formate–acetate–propionate. In the same sequence, the content of pyrolytically formed carbon in the decomposition products increases. In case of acetates and propionates a thermal hydrolysis process forming the corresponding carboxylic acids already begins below the boiling point of the acid. This results in a partial separation of components in the former homogeneous precursor. The worse homogeneity involves a higher temperature for the synthesis of single-phase complex oxides. Moreover, the intermediate occurrence of fluid suspensions leads to hard agglomerated solids. In case of formate decomposition, the release of formic acid begins only above the boiling point and loose, soft agglomerated powders are formed.

Acknowledgements

The authors gratefully acknowledge financial support by the Deutsche Forschungsgemeinschaft and the Fonds der Chemischen Industrie.

References

[1] Kh.M. Yakubov, V.A. Logvinenko, T.A. Zhemchuzhnikova, Sh.Kh. Abdullaev, G.V. Gavrilova, A.N. Mikheev, J. Thermal Anal. 30 (1985) 1095.
[2] L. Patron, A. Contescu, G. Munteanu, M. Brezeanu, E. Segal, Rev. Roum. Chim. 31 (1986) 811.
[3] I. Ilie, M. Brezeanu, L. Patron, E. Segal, G. Filoti, Rev. Roum. Chim. 32 (1987) 1109.
[4] I. Ilie, M. Brezeanu, L. Patron, E. Segal, Rev. Roum. Chim. 33 (1988) 803.
[5] A.B. Blake, A. Yavari, W.E. Hatfield, C.N. Sethulehshmi, J. Chem. Soc., Dalton Trans. 12 (1985) 2509.
[6] Ch.T. Dziobkowski, J.T. Wrobleski, Inorg. Chem. 20 (1981) 679.
[7] H. Langbein, P. Eichhorn, Z. Chem. 30 (1990) 4.
[8] H. Langbein, C. Michalk, K. Knese, P. Eichhorn, J. Eur. Ceram. Soc. 8 (1991) 171.
[9] S. Christen, H. Langbein, K. Jaenicke-Rößler, Thermochim. Acta 209 (1992) 253.
[10] D. Dollimore, K.H. Tonge, J. Inorg. Nucl. Chem. 29 (1967) 621.
[11] I. Barin, Thermodynamic Data of Pure Substances, VCH Verlagsgesellschaft mbH, Weinheim, 1989.
[12] G. Bonsdorf, K. Schäfer, K. Teske, H. Langbein, H. Ullmann, Sol. Stat. Ionics 110 (1998) 73.